ELSEVIER

Polymer 40 (1999) 5609–5621

polymer

Coalescence in PC/SAN blends: effect of reactive compatibilization and matrix phase viscosity

G. Wildes, H. Keskkula, D.R. Paul*

Department of Chemical Engineering and Center for Polymer Research The University of Texas at Austin, Austin, TX 78712, USA

Received 16 April 1998; received in revised form 27 October 1998; accepted 28 October 1998

Abstract

This study introduces a technique developed for the quantitative measurement of the kinetics of dispersed phase particle coalescence in polymer blends. The method has been shown to be useful and reproducible for the study of morphology development and stability in polymer melt blending. Using this technique, we examined the relative importance of reactive compatibilizers, shear history and matrix phase viscosity on the morphological stability of PC/SAN blends. © 1999 Elsevier Science Ltd. All rights reserved.

Keywords: PC; SAN; Polymer blend

1. Introduction

Multiphase polymer blends have become commercially important for a variety of applications (e.g., automotive, electronics, etc.) and one of the most successful of these is mixtures of bisphenol-A polycarbonate with acrylonitrile–butadiene–styrene materials, i.e., PC/ABS [1–5]. A significant body of literature has examined the thermodynamics, morphology and properties [3–16] of these blends; a few articles have examined the morphological rearrangements of this system during quiescent periods in the melt state [12,17–19].

Compatibilization of blends by the incorporation of appropriate block or graft copolymers reduces the interfacial tension and retards the coalescence processes via steric stabilization; this makes it easier to achieve a finer dispersion of the dispersed phase, increases the interfacial strength, and improves the stability of the morphology in the melt state. Relatively small and uniformly dispersed phase particles are usually advantageous for the properties of polymer blends; generally ABS materials can be adequately dispersed in polycarbonate by conventional extrusion compounding without the use of compatibilization [3,12,15,17] caused by the nearly favorable interactions between PC and the styrene–acrylonitrile copolymer, SAN, matrix [6]. Indeed, uncompatibilized PC/ABS blends are successful commercial materials that have exceptional low temperature toughness [1–5,16]. However, these uncompatibilized PC/ABS blends undergo significant dispersed phase particle coalescence in the melt state under certain molding conditions, and this leads to a significant deterioration of the properties of the blend. Thus, minimizing this limitation might extend the commercial opportunities for PC/ABS blends. Reactive compatibilization has been shown to effectively stabilize the morphology of other polymer blend systems [20–28]. The goal of this article is to show that a reactive compatibilization scheme proposed for PC/ABS in a previous article [29] does improve the stability of the morphology of blends of PC with the styrene–acrylonitrile copolymer matrix of ABS materials.

2. Background

The development and stability of the morphology of multiphase polymer melts is a complex function of blend composition, interfacial characteristics, rheological properties, and shear conditions [28,30–42], and perhaps other attributes of the constituent materials. The competing processes of drop break-up and coalescence during processing of polymer blends determine the final morphology of these mixtures as explained in a growing body of literature on this subject [21–27,43–45].

2.1. Drop break-up

In the early 1930s, Taylor developed a theory for the

* Corresponding author. Tel.: + 1-512-471-5392; fax: + 1-512-471-0542.

E-mail address: paul@che.utexas.edu (D.R. Paul)

PII: S0032-3861(98)00776-9

break-up of individual droplets for Newtonian fluids [46,47]. A relationship was established between the capillary number, Ca, a ratio of shear to interfacial forces,

$$\mathrm{Ca} = \frac{G\eta_m d}{2\gamma} \tag{1}$$

and the viscosity ratio, $\eta_r = \eta_d/\eta_m$, where G is the shear rate, d is the diameter of the droplet, γ is the interfacial tension, η_d is the dispersed phase viscosity, and η_m is the matrix phase viscosity. The predicted drop size for a simple shear field is proportional to the interfacial tension and inversely proportional to shear rate and matrix phase viscosity. This theory applies to systems with vanishingly small concentrations of the dispersed phase and drop break-up is predicted to occur only for systems when $\eta_r < 2.5$. Other experimental studies have confirmed these results with qualitative agreement of data for simple shear and have shown that the particle size dependence on viscosity ratio exhibits a minimum between $\eta_r = 0.1$ *and* 1.0 [48–51]; extensional flow has been shown to be more effective for inducing drop break-up over a much wider range of viscosity ratios. Extruders and compounding mixers impose a mixture of both shear and extensional flows on the polymer melt.

Although Newtonian systems are relatively well understood, there are many limitations of Taylor's theoretical framework for predicting the morphology of a multiphase macromolecular system [52,53]. In addition to viscoelastic effects, other difficulties in comparing such ideal systems to polymer blends include the complex shear fields encountered in processing and the relatively high concentrations of the dispersed phase in commercial polymeric materials.

2.2. Coalescence

Commercially useful multiphase blends may exhibit significant dispersed phase particle coalescence [22–24,30,31,44,54] both during flow and quiescent conditions that exist in melt fabrication processes. Von Smoluchowski developed much of the early theoretical framework for studying coalescence phenomena in colloidal solutions [55,56]. Later, Tokita used this theory to equate the rate of coalescence derived by von Smoluchowski to an expression for the rate of drop break-up during processing, resulting in an equation for calculating the equilibrium particle size in polymer blends. When the rates of drop break-up and coalescence are in dynamic equilibrium, the relation predicts that the particle size decreases as applied stress increases and the interfacial tension between the phases decreases. The dispersed phase particle size increases as the dispersed phase concentration increases, indicating the effect of coalescence during processing of concentrated systems.

To quantify particle coarsening in polymer blends, most studies have examined materials in a quiescent state. Under these conditions, diffusion dependent phenomena have been shown to significantly underestimate the rate and extent of particle coarsening in polymeric systems [54,57–60] caused by the high viscosities and extremely low mutual solubilities of polymer–polymer pairs. Particle coarsening caused by coalescence phenomena of dispersed phase domains in polymer–polymer systems has been studied in a number of recent works [17–19,21–24,27,32,43,44,59,61–66]. For two particles to fuse, they must first come into close proximity of each other by some flow process driven by a shear field, hydrodynamic interaction, gravity, or other force. Once two particles are in near contact, there is only a finite chance that coalescence of the particles will occur. This coalescence probability depends, among other variables, on the viscosity of the matrix phase, as there must be sufficient time to allow for drainage of the film between the dispersed phase domains [23,24,27,44]. Therefore, the extent of coalescence is a net product of the probability of particle contacts and the probability that any one of those contacts has sufficient matrix film drainage to allow for particle fusion. Because of the first stage in this sequence, coalescence can be flow induced.

Recent studies have shown that the dispersed phase particle size developed during processing can increase, decrease, or show complex non-monotonic behavior as the shear rate is increased [22,23,66] because of the competing effects of increased particle–particle contacts versus decreased contact times. Changes in polymer elasticity at high shear rates may also affect the dynamic equilibrium between particle break-up and coalescence.

2.3. Compatibilization of PC/ABS

Compatibilization by the addition (or in situ formation) of block or graft copolymers provides improved morphological stability by lowering the interfacial tension and, perhaps more importantly, introducing a steric hindrance to coalescence [21,22,27,44,67]. Recently, Macosko et al. proposed that the theoretical surface coverage of block copolymer compatibilizers required for steric stabilization of PS/PMMA blends is, [20]

$$\Sigma_c \frac{20}{27\pi\langle r_o^2\rangle}, \tag{2}$$

where $\langle r_o^2\rangle$ is the mean square of the end-to-end distance of the unperturbed compatibilizer chain. A blend that contains a volume fraction ϕ_d of dispersed phase spherical particles with diameter d has an interfacial area per unit volume of $6\phi_d/d$. If it is assumed that all compatibilizer molecules added to the system reside at the polymer/polymer interface, the concentration of these molecules per unit interfacial area is given by,

$$\Sigma_c = \frac{\text{molecules/vol}}{\text{interface area/vol}} = \frac{N_A\rho_c\phi_c d}{6M_c\phi_d}, \tag{3}$$

where N_A is Avagadro's number, ρ_c is the polymer density,

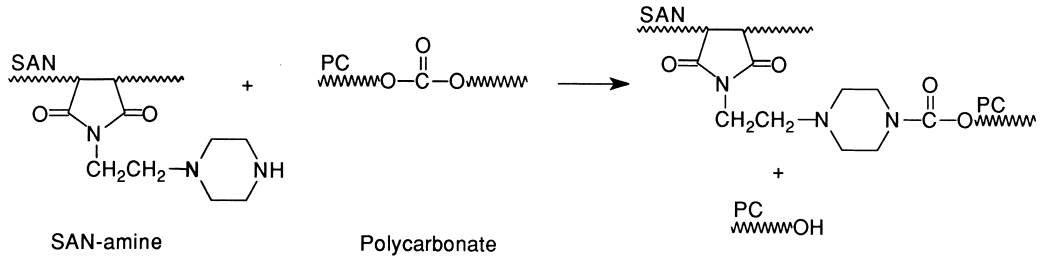

Fig. 1. Schematic of the reaction of SAN-amine with bisphenol-A-polycarbonate to form SAN-g-PC [29].

ϕ_c is the fraction of compatibilizer, and M_c is the molecular weight of the compatibilizing polymer.

Schemes for formation of block and graft copolymer by in situ reactions during melt processing are well-known for blends based on polyamides and polyesters which utilize their amine, carboxyl or hydroxyl functional chain ends. However, most commercial polycarbonates do not have reactive chain ends as they are generally capped during polymerization to obtain more stable and color-free products [68]. In a recent article, we introduced a novel chemical approach for the compatibilization of PC/ABS blends [29]. The formation of SAN-g-PC copolymer at the PC/SAN interface is accomplished through the chemical scheme shown in Fig. 1. The SAN-amine polymer is synthesized by reacting a styrene/acrylonitrile/maleic anhydride (67/32/1) terpolymer with 1-(2-aminoethyl) piperazine in a reactive processing scheme. The SAN-amine polymer is miscible with the SAN matrix of ABS and reacts with PC as shown. The graft copolymer formed has been shown to reduce the SAN dispersed phase particle size in a fixed mixing process. The purpose here is to examine the stability of this morphology using a novel technique introduced here and in another recent article [69]. This involves preparing a blend in a batch mixer at a high rotor speed until an equilibrium particle size distribution is established. The rotor speed is then reduced to a low level allowing the extent and rate of particle coarsening to be measured as a function of time; in an unstable system the particle size would grow over time owing to the reduced rate of drop break-up relative to the ratio of coalescence.

3. Experimental

3.1. Materials

The composition and suppliers of the polymers employed in this work are shown in Table 1. The designation for each commercial polycarbonate is based on its relative molecular weight; high (H-PC), medium (M-PC) and low (L-PC). A commercial SAN copolymer containing 32.5% AN, SAN32.5, was used; the functionalized SAN-amine polymer has been described in a previous article [29]. All materials were dried in a vacuum oven at 80°C for at least 12 h before melt processing. Melt mixing was done in a Brabender Plasticorder at 270°C and 60 rpm, except where noted, with a 50 cm^3 mixing head and standard rotors. Fig. 2 shows Brabender torque as a function of temperature for commercial polycarbonates and ABS materials. Melt blending below the processing window indicated on Fig. 2 results in larger viscosity differences between the dispersed and matrix phases while processing above this temperature range can lead to significant degradation of the rubber phase in ABS. Therefore, 270°C was selected as the operating temperature. At this temperature, the various polycarbonate materials used in this study represent a wide range of viscosities as seen in Fig. 3. Only SAN materials without a rubber phase were blended with polycarbonate to study morphology stability. This choice represents a simple model of PC/ABS blends that facilitates the quantitative analysis of dispersed phase particle sizes while eliminating some of the problems of rubber phase degradation during the long processing times used here.

3.2. Brabender methodology

Sixty grams of pre-mixed polymer pellets were added to the preheated Brabender mixing chamber over approximately 15–20 s after which the blend was fluxed for specified times and rotor speeds. After approximately 7–8 min of mixing at 270°C and 60 rpm, an equilibrium particle size was established. This average particle size showed very little difference between samples taken at 10, 20 and 30 min of mixing. To study coalescence, the rotor speed was reduced to 5 rpm after 10 min of mixing at 60 rpm. The low (non-zero) shear rate was chosen to provide an increased probability, compared to a quiescent (zero shear rate) state, of SAN phase particle–particle collisions.

Small samples were taken from the Brabender chamber with metal spatulas after the rotor was stopped and the top chamber cover was removed, sampling time was about 5–10 s. A 1.5–2.5 g sphere of polymer melt was removed from between the rotors with care being taken not to elongate or orient the sample to avoid altering the blend morphology. The sample was immediately quenched in a stirred 8 l ice water bath. By experimentally embedding a thermocouple in a 3 g sphere of PC/ABS (70/30), it was found that the sample center was effectively quenched from the melt to below the glass transition of polycarbonate, 151°C, in approximately 25 s. This should be an upper bound for the

Table 1
Polymers used in this study

Polymer Trade name	Designation	Description	$\overline{M}_w$	$\overline{M}_n$	Torque (N m)[a]	Relative melt viscosity	Source
PC E2000	H-PC	BPA polycarbonate High MW	32,000	10,800	13.10	4.37	Mitsubishi Engineering Plastics Corporation
PC S3000	M-PC	BPA polycarbonate Medium MW	23,700	8,500	7.70	2.57	Mitsubishi Engineering Plastics Corporation
PC H3000	L-PC	BPA polycarbonate Low MW	20,100	7,400	4.55	1.52	Mitsubishi Engineering Plastics Corporation
SAN Lustran35	SAN32.5	Styrene acrylonitrile copolymer, 32.5% AN	130,000	59,000	3.00	1.00	Bayer Corporation
SAN SAN-amine	SAN-amine	Amine functional S/AN/amine (67/32/1)	117,300	48,100	3.90	1.30	Bayer Corporation
ABS Magnum541	ABS-D16	16% Rubber 25% AN in SAN	140,000	59,000	3.90	1.33	Dow Chemical Company
ABS Lustran38	ABS-B38	38% Rubber 30% AN in SAN	130,000	59,000	10.00	3.33	Bayer Corporation
ABS SAN-g	ABS-C45	45% Rubber 25% AN in SN	90,000	35,000	12.70	4.2	Cheil Industries
ASA Geloy	ASA-G46	46% Acrylate rubber 33% AN in SAN	NA		9.6	2.7	GE Plastics

[a] Brabender torque taken after 10 min mixing at 270°C and 60 rpm.

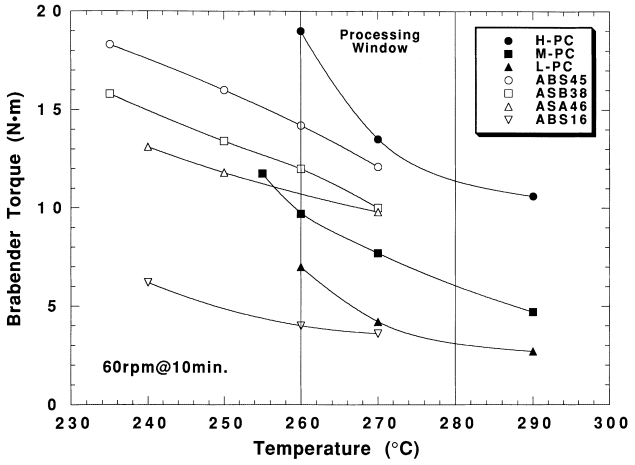

Fig. 2. Brabender torque vs temperature for the polymers used in this study (torque at a rotor speed of 60 rpm after 10 min mixing).

quench time as the 3 g sample was slightly larger than those used in this study.

3.3. TEM analysis

Transmission electron microscopy (TEM) was used to examine the morphology of the melt processed blends of PC/SAN and PC/SAN/SAN-amine. Cryogenically microtomed sections, about 20 nm thick, were prepared with a Reichert-Jung Ultracut E at a sample temperature of −10°C (−45°C knife). Brabender specimens were microtomed with a diamond knife parallel to the sample surface at a depth of approximately 2 mm from the surface. The sample morphology was generally orientation independent (±10%) at a specified depth in the sample.

The polycarbonate phase of the blends was preferentially stained by exposing the ultra-thin sections to the vapors of a 0.5% aqueous solution of RuO_4 at room temperature. TEM imaging was done on a Jeol 200CX microscope operating at 120 keV. The apparent particle diameter was determined by digitizing TEM photomicrographs; the diameter of an equivalent circle having the same area as a scanned particle was defined as the particle diameter. No corrections were applied to the calculated diameters because of the non-spherical nature of many of the particles. Correction methods described in the literature do not apply to complex shapes [70,71] such as those seen in many of the morphologies for this study. The weight average particle diameter, $\bar{d}_w$,

$$\bar{d}_w = \frac{\Sigma n_i d_i^2}{\Sigma n_i d_i}$$

of the dispersed phase was calculated from an analysis of 100 to 800 particles taken from multiple TEM photomicrographs employing NIH Image® 1.60 digital image analysis software.

4. Low shear rate coalescence in PC/SAN blends

4.1. Effect of shear history

The effect of shear rate on the dynamic equilibrium between dispersed phase particle break-up and coalescence during processing was qualitatively examined by selectively changing the Brabender rotor speed. Fig. 4 shows the rotor speed and torque of a M-PC/SAN32.5 (70/30) blend for an experiment in which the Brabender mixer was run at 60 rpm for 10 min, followed by a low shear period at 5 rpm for 5 min, followed by an additional 5 min at 60 rpm. The lower shear rate used in this experiment should result in less effective particle break-up and longer dispersed phase particle–particle contact times. The TEM photomicrographs in Fig. 5 correspond to the sampling of the melt blend as indicated in Fig. 4 at points a, b, c and d.

Figs 5(a) and (b) show TEM photomicrographs of the morphology of a 70/30 blend of M-PC/SAN32.5 as a function of melt mixing time; the letter designates mixing times of 5 min and 10 min, respectively, corresponding to

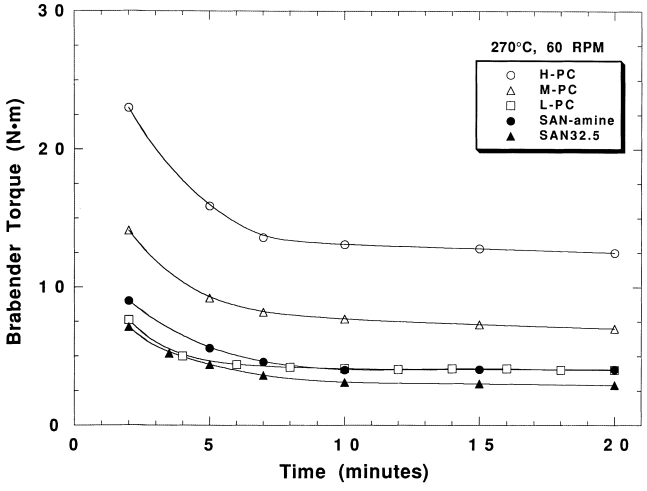

Fig. 3. Brabender torque vs. time for the polymers used in this study (270°C at a rotor speed of 60 rpm).

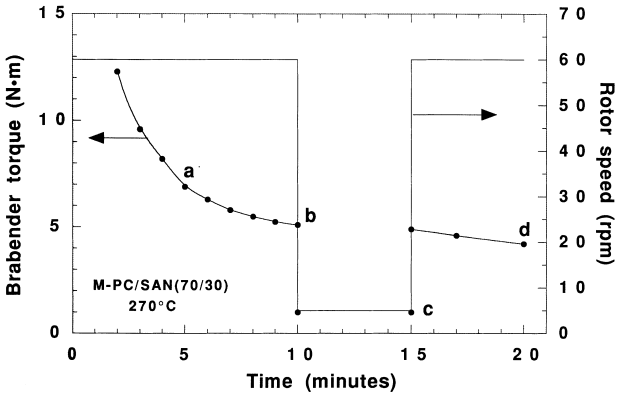

Fig. 4. Brabender torque and rotor speed vs. time for investigation of drop break-up and coalescence in a M-PC/SAN25 (70/30) blend, samples were taken at locations a, b, c and d for TEM analysis.

points a and b in Fig. 4; with more mixing time the large SAN domains become smaller. After approximately 7–8 min of mixing at 270°C and 60 rpm, an equilibrium particle size was established. Some of the phenomena involved in drop break-up can be seen in Fig. 5a; the large domains are in the form of elongated phases which lead to the formation of smaller droplets caused by capillary instabilities in the extended regions. After 10 min of mixing, the three-dimensional morphology was determined to be spheroidal SAN domains dispersed in the PC matrix with no evidence of elongated dispersed phase structures. (see Fig. 5b). At the low shear rate, the growth in size of the SAN domains caused by coalescence can be seen by comparing Figs. 5b and c (notice the disappearance of the smallest domains). After increasing the shear rate again, some of the large coalesced SAN domains remained while others were broken

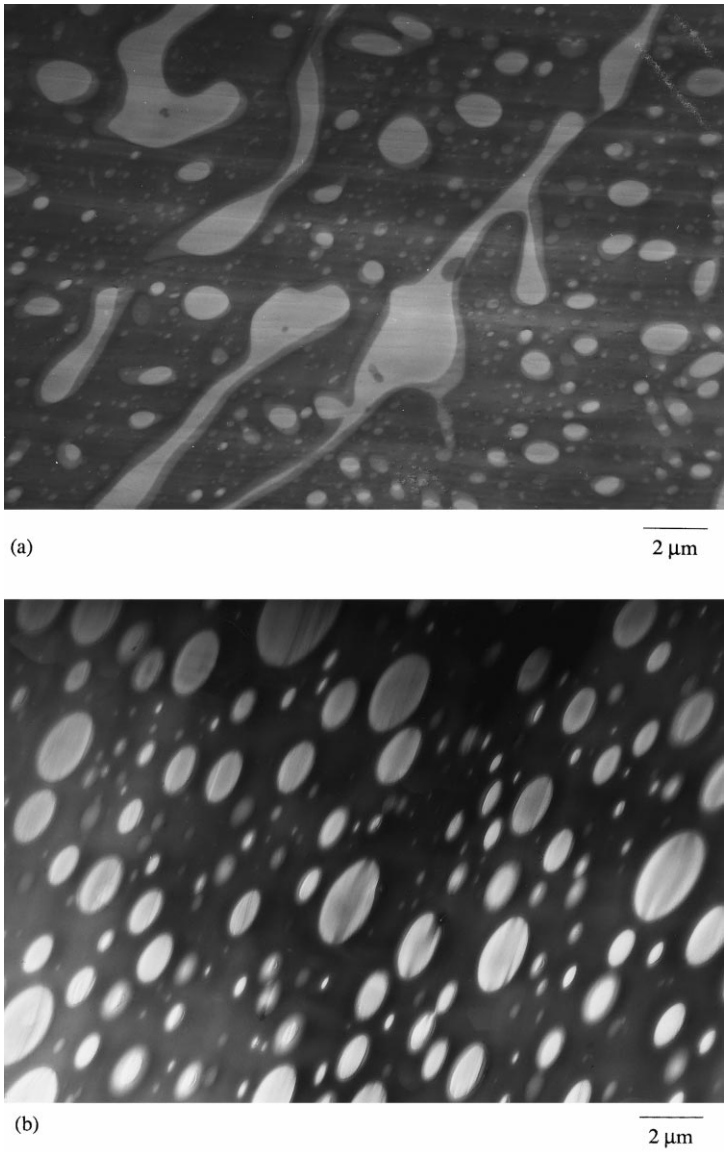

Fig. 5. TEM photomicrographs for M-PC/SAN25 (70/30) blend mixed in a Brabender at 270°C as indicated in Fig. 4, stained with RuO_4 (a) 5 min at 60 rpm, (b) 10 min at 60 rpm, (c) 10 min at 60 rpm + 5 min at 5 rpm, (d) 10 min at 60 rpm + 5 min at 5 rpm + 5 min at 60 rpm.

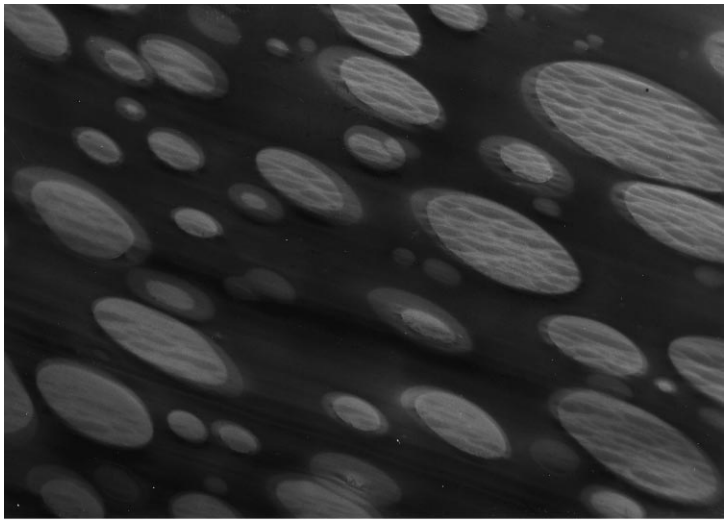

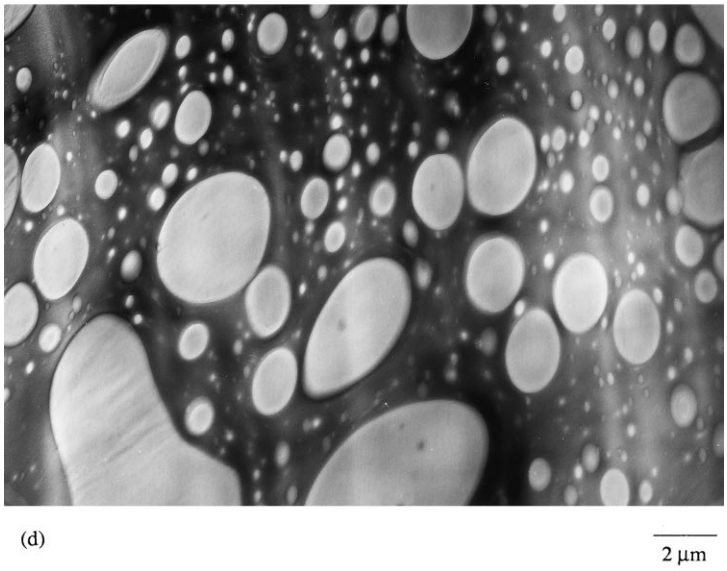

Fig. 5. (*continued*)

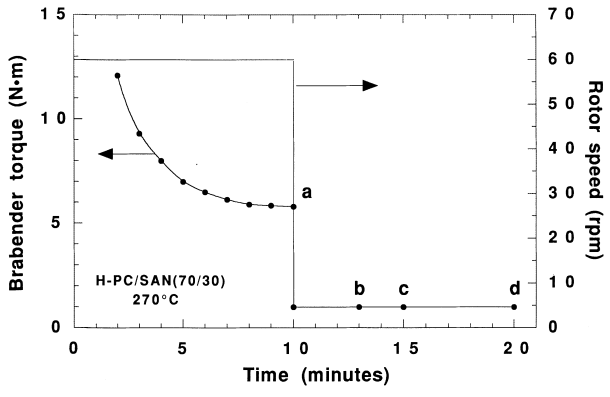

Fig. 6. Brabender torque and rotor speed vs. time for the investigation of H-PC/SAN32.5 (70/30) blend coalescence, samples were taken at a, b, c and d for TEM analysis.

into small droplets, (see Fig. 5d), creating a broad particle size distribution.

4.2. Kinetics of blend coalescence

As a result of the different balance between break-up and coalescence processes, a larger average particle size will evolve when the rotor speed is reduced to 5 rpm from 60 rpm. The growth in particle size caused by coalescence can be followed as a function of time by analyzing samples taken after this step change in rotor speed. Samples from the H-PC/SAN32.5 (70/30) melt blend were taken after 0 (a), 3 (b), 5 (c) and 10 (d) minutes, as indicated in Fig. 6, to establish the time dependence of the particle size as it approaches a new equilibrium value. Fig. 7a shows the equilibrium morphology obtained for the blend after

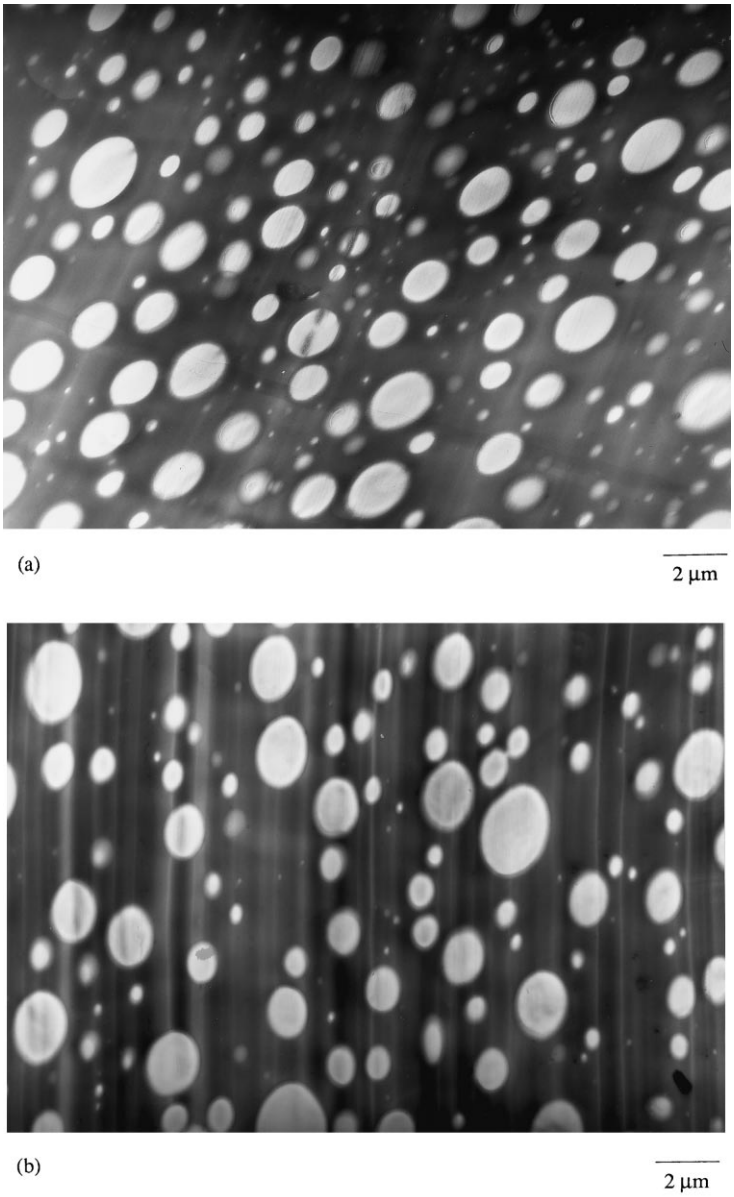

Fig. 7. TEM photomicrographs for H-PC/SAN32.5 (70/30) blend mixed in a Brabender at 270°C as indicated Fig. 6, stained with RuO_4(a) 10 min at 60 rpm, (b) 10 min at 60 rpm + 3 min 5 rpm, (c) 10 min at 60 rpm + 5 min at 5 rpm, (d) 10 min at 60 rpm + 10 min at 5 rpm.

10 min of mixing. Some limited SAN phase coarsening is evident in Fig. 7b after 3 min at the low shear rate. However, after 5 min at 5 rpm, Fig. 7c shows a much larger particle size compared to Fig. 7a. In fact, there were two different morphologies seen in this system after 5 min; some areas looked similar to Fig. 7b while other areas, seen in Fig. 7c, showed large elongated domains recently formed by coalescence. In Fig. 7d, there is a larger average particle size than seen at earlier times at 5 rpm and there are no "very small" particles.

The average dispersed phase particle sizes (with error bars of plus and minus one standard deviation of the particle size distribution) are plotted as a function of time in Fig. 8. Time zero corresponds to the reduction in rotor speed from 60 rpm to 5 rpm (10 min after the addition of the mixed pellets to the mixing chamber). As seen in Fig. 8, the morphology at low shear rate is a strong function of time for uncompatibilized blends. The high rate of coalescence of this blend resulted in a significant increase in particle size during the first 5 min. Although the particle size increases during the period from 5 to 7 min, the particle size distribution actually becomes more narrow as the elongated SAN domains become mostly spherical in shape. After the increase in particle size during the first 5 min, the rate of particle coarsening slowed leading to an approach to a new equilibrium size. A similar time dependence of dispersed phase particle size during quiescent coalescence for PC/SAN (70/30) blends was seen in two other articles [12,17].

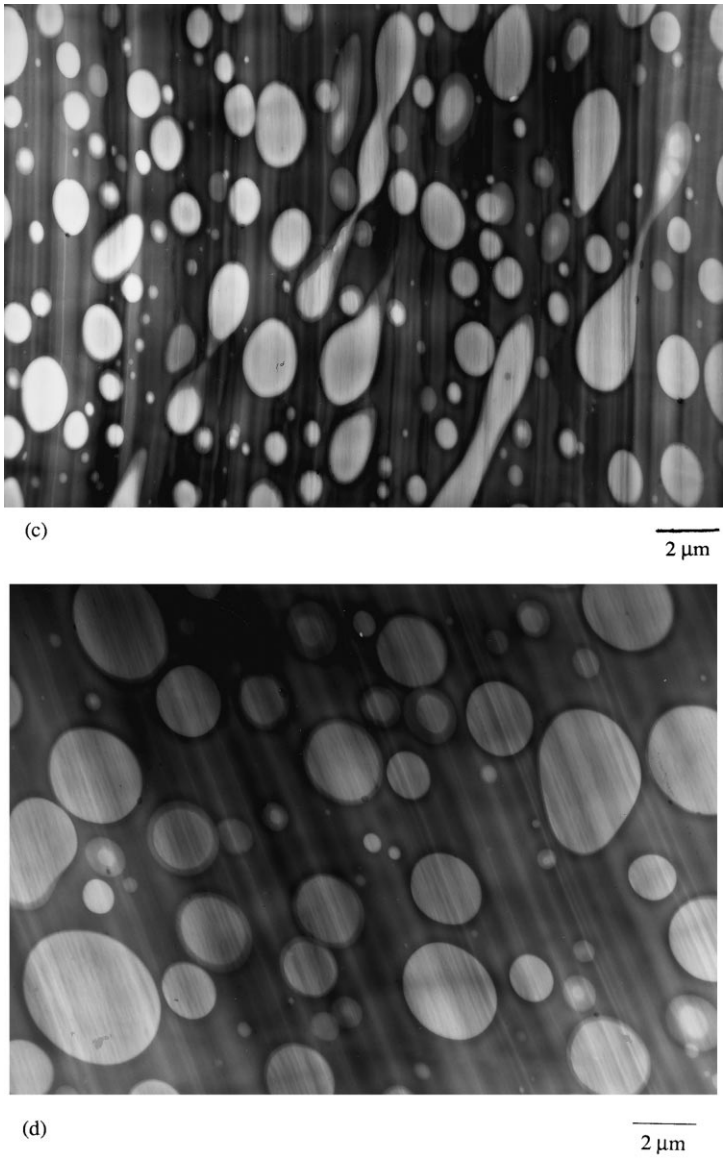

Fig. 7. (*continued*)

4.3. Effect of matrix viscosity

As previously discussed, the matrix viscosity plays a key role in the time required for film drainage between two drops of the dispersed phase which affects the overall rate of coalescence for a given blend system. Other studies have shown that increased matrix phase viscosity reduces coalescence [72,73]. The effect of matrix viscosity on the kinetics of coalescence for PC/SAN blends is significant as seen in Fig. 9. Not only is the average dispersed phase particle size significantly larger for the lower molecular weight polycarbonate matrices, but the initial rate of particle coarsening is greater as well. There is a substantial difference in the rates of coarsening for H-PC compared to both M-PC and L-PC; however, there is little difference in the extent and rate of coalescence between these lower molecular weight polycarbonates.

The unexpectedly high coalescence rates of viscous polymer–polymer blends might partially be explained by the fact that viscosities exhibited by thin polymer films are significantly lower than those measured for the bulk polymer [74,75]. It has been suggested that the lower localized matrix viscosity would facilitate film drainage and increase the probability for coalescence [24]. To the knowledge of these authors, such an effect of thin film viscosity has not been taken into account in theoretical studies of the rate of coalescence.

4.4. Effect of reactive compatibilization

The same experiments described in Fig. 6 were carried out for the corresponding compatibilized blend, H-PC/SAN32.5/SAN-amine (70/20/10), see Fig. 10. Most compatibilized blends show significantly higher melt viscosities

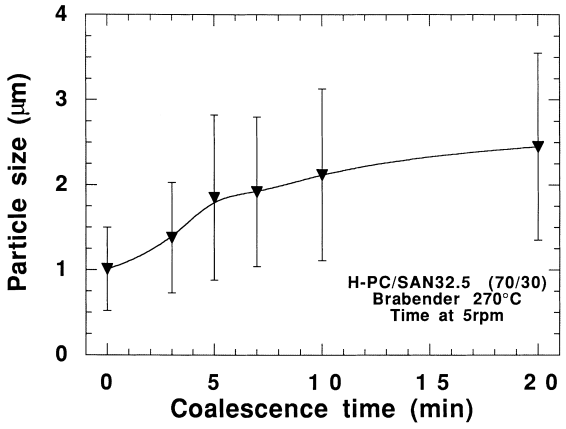

Fig. 8. Average dispersed phase particle size (±one standard deviation of the particle size distribution) for H-PC/SAN32.5 (70/30) blend as a function of coalescence time at 5 rpm ($t = 0$ corresponds to a blend mixed in a Brabender for 10 min at 60 rpm).

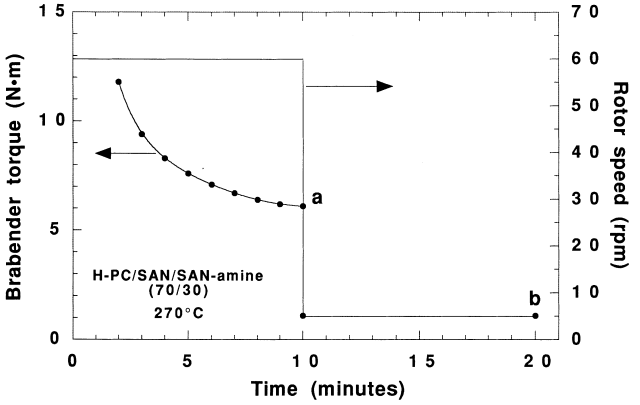

Fig. 10. Brabender torque and rotor speed vs. time for investigation of H-PC/SAN32.5/SAN-amine (70/20/10) compatibilized blend, samples taken at a and b for TEM analysis.

than comparable uncompatibilized systems [76,77]; however, the torque response for the compatibilized PC/SAN system was only slightly higher than for the uncompatibilized blend, compare Figs. 6 and 10. This is explained by the PC chain scission that accompanies grafting to the compatibilizer molecule when the carbonate unit reacts with the secondary amine functionality of SAN-amine. The reaction results in two macromolecules, a relatively large SAN-g-PC molecule and a lower molecular weight PC chain, which causes competing effects on the viscosity of the blend, especially at high shear rates.

Fig. 11 shows that the SAN phase particle size is significantly smaller for the compatibilized blend relative to uncompatibilized PC/SAN, compare Fig. 7a and Fig. 11a. In addition, the SAN particle size is substantively the same in Figs. 11a and b; 10 min at the low rotor speed apparently does not lead to significant coalescence in the compatibilized blend.

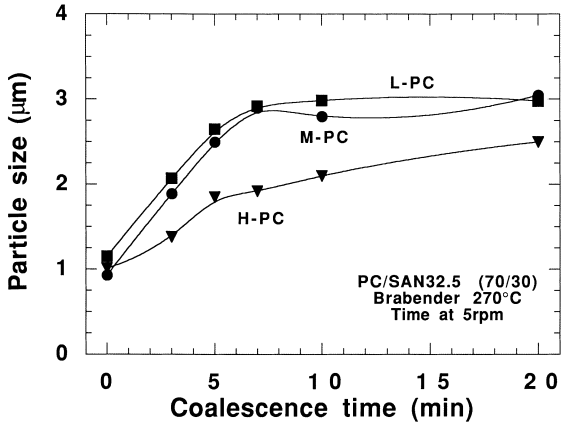

Fig. 9. Comparison of kinetics of coalescence for H-PC, M-PC and L-PC in PC/SAN32.5 (70/30) blends mixed at 270°C and 60 rpm for 10 min followed by slow mixing at 5 rpm.

Quantitative analysis of the morphologies in Figs. 7 and 11 is shown in Fig. 12. The uncompatibilized blend of H-PC with SAN32.5 has a particle size distribution which broadens significantly after 10 min at low shear conditions while the compatibilized blend only broadens slightly and shows no particles larger than 1.25 μm. The dramatic difference in morphological stability seen in Fig. 12 could be caused by an immobilization of the polymer–polymer interface caused by the presence of the SAN-g-PC at the polymer–polymer interface. While most polymer blends are expected to have mobile interfaces which facilitate film drainage during coalescence, interfacial compatibilizers may prevent coalescence by immobilizing the interface [44].

Numerous experiments were carried out to quantify the variance in average calculated particle sizes obtained by using the previously described techniques. Fig. 13 shows the results of these experiments for uncompatibilized and compatibilized blends of H-PC/SAN32.5/SAN-amine (70/30 − X/X). The data points in Fig. 13 represent the average dispersed phase particle size measured from more than 30 separate experiments, thus establishing the repeatability of this technique for studying coalescence in polymer blends. Fig. 13 elucidates the stability of the compatibilized blends, even at very low concentrations. The results of varying the SAN-amine content in these blends is plotted in Fig. 14. Apparently, under these processing conditions, a very small amount of SAN-amine has a significant effect on the morphology of PC/SAN blends, especially its stability. Other studies have also shown that only very small concentrations of compatibilizer are necessary for significant modification of the polymer–polymer interface in immiscible blend systems [22,27,28].

The criteria proposed by Macosko et al. [20] can be used to estimate the minimum amount of compatibilizer needed to achieve steric stabilization. Equating Σ from Eq. (2) to Σ_c from Eq. (3) results in the following expression for the

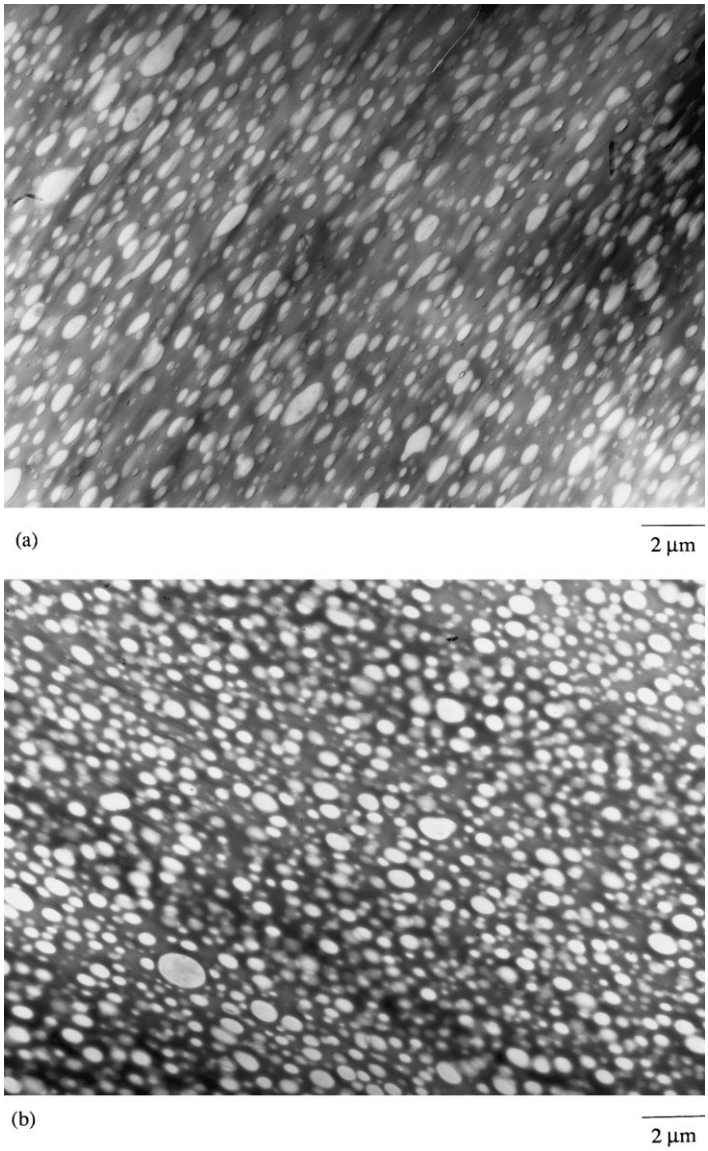

Fig. 11. TEM photomicrographs for H-PC/SAN32.5/SAN-amine (70/20/10) blend mixed in a Brabender at 270°C as indicated in Fig. 10, stained with RuO_4 (a) 10 min at 60 rpm and (b) 10 min at 60 rpm + 10 min at 5 rpm.

minimum required compatibilizer concentration

$$\phi_c = \frac{(20 \times 6/27\pi N_A)(\phi_d/\rho_c d)}{(\langle r_o^2 \rangle / M_c)}. \quad (4)$$

Using a value of $\langle r_o^2 \rangle / M_c$ of 6.6×10^{-3} (nm^2) estimated from published values for the SAN backbone [78] of the SAN-g-PC graft copolymer, $d = 0.5$ μm, $\phi_d = 0.3$, and $\rho_c = 1.1$ g/cm^3 leads to an estimate of $\phi_c = 2 \times 10^{-4}$. This is approximately 50 times the lowest concentration used in this study. It has been suggested that the amount of compatibilizer surface coverage necessary for stabilizing blend morphologies during static coalescence may be significantly higher than the concentrations required during mixing [20], possibly caused by longer contact times which allow for a greater extent of molecular rearrangement at the interface.

5. Conclusions

The batch mixer (Brabender) methodology developed in this study provides a useful and reproducible means for quantitative examination of morphological development and stability in polymer blends. The technique involves preparing a blend in a batch mixer at a high rotor speed until an equilibrium particle size distribution is established. The rotor speed is then reduced to a low level allowing the extent and rate of particle coarsening to be measured as a function of time. Particle coarsening in the uncompatibilized PC/SAN (70/30) blends was found to be substantial over a time frame of about 5 min; $\bar{d}_w$ increased from 1 to 2 μm. After 5 min of coalescence time, large elongated dispersed phase domains were evident and the rate of coarsening decreased with the particle size growing to about

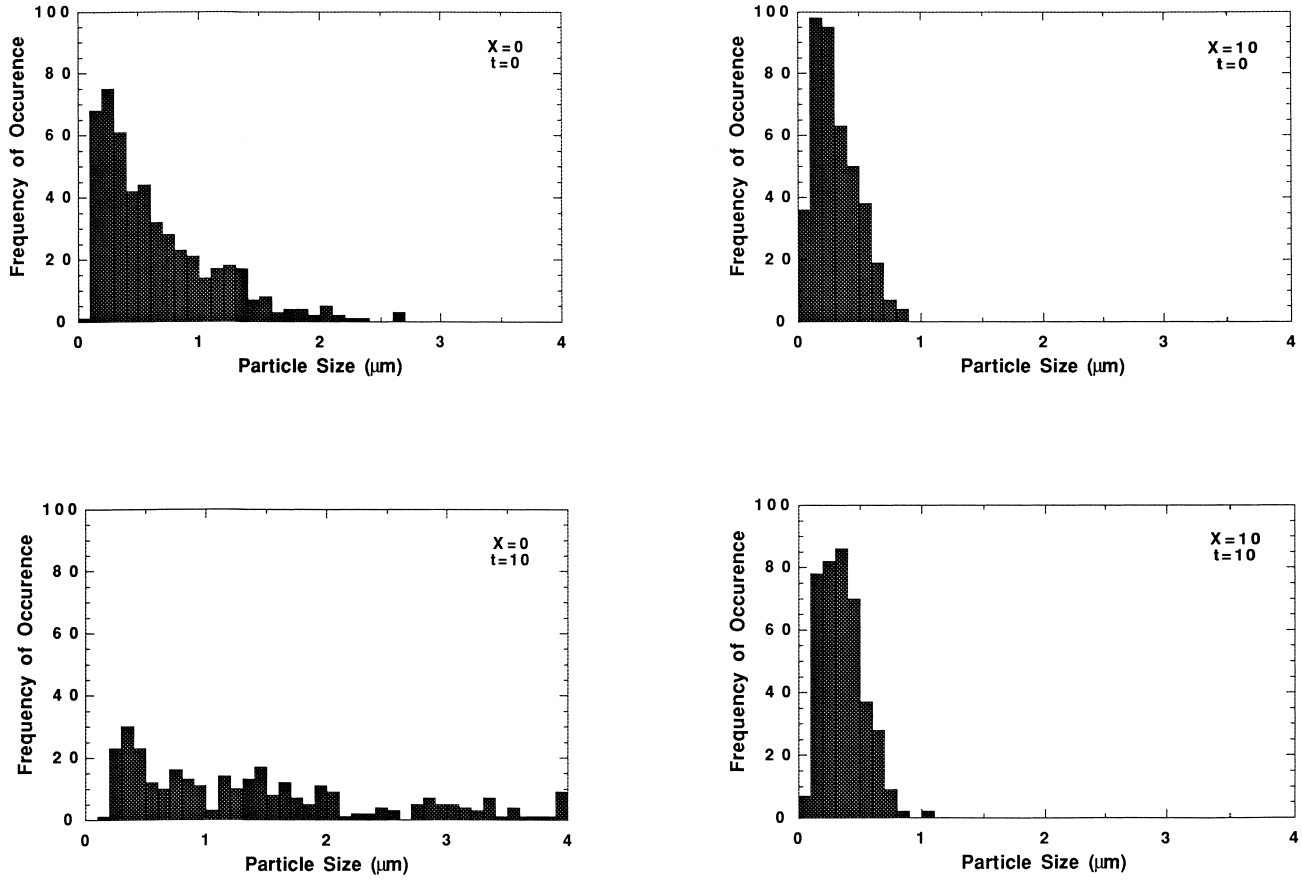

Fig. 12. Particle size distributions for H-PC/SAN32.5 (70/30) ($X = 0$) and H-PC/SAN32.5/SAN-amine (70/20/10) ($X = 10$) after 10 min at 60 rpm ($t = 0$) and 10 min at 60 rpm + 10 min at 5 rpm ($t = 10$), X is the SAN-amine concentration and t is the coalescence time.

2.5 μm after 20 min at the low shear rate. Lower matrix phase viscosities resulted in somewhat faster coalescence. Compatibilized blends, using a functionalized SAN-amine polymer, were found to have smaller SAN particle sizes (0.5 μm) and to show no significant dispersed phase coalescence, even after 20 min at 270°C. The SAN-amine compatibilizer was effective even at very low concentrations. This technique is currently being used to compare the morphological stability of compatibilized and uncompatibilized blends in other polymer systems.

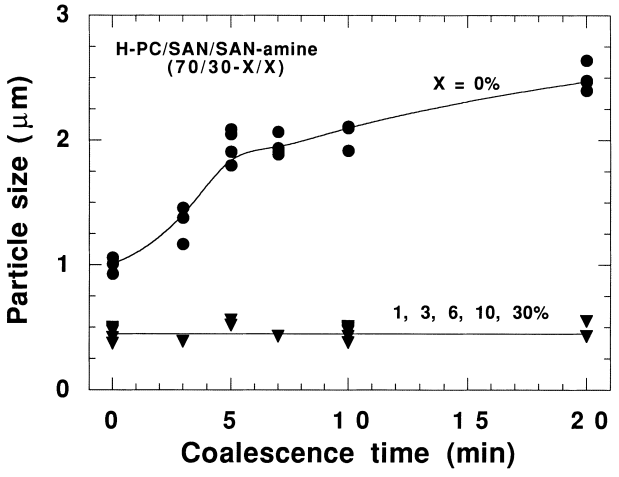

Fig. 13. Kinetics of coalescence and repeatability of particle size data for H-PC/SAN32.5 (70/30) ($X = 0$) and H-PC/SAN32.5/SAN-amine (70/30 − X/X) blend ($X = 1, 3, 6, 10$).

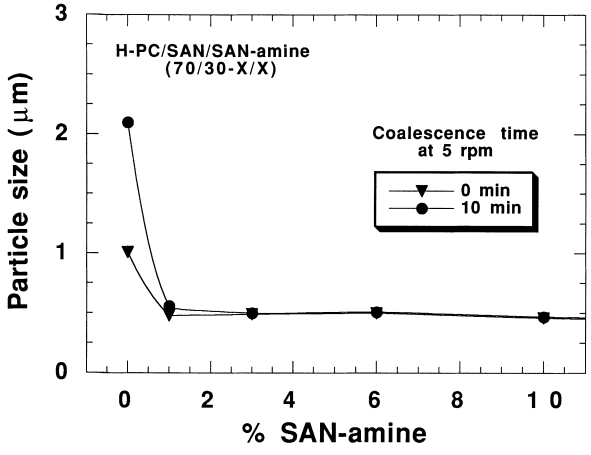

Fig. 14. Extent of coalescence in compatibilized and uncompatibilized blends of H-PC/SAN32.5/SAN-amine (70/30 − X/X) mixed in a Brabender at 270°C, particle size data taken after 10 min at 60 rpm and 10 min at 60 rpm + 10 min at 5 rpm.

Acknowledgements

This research was supported by the US Army Research Office under an AASERT grant. G.S.W. is grateful for a supplemental research fellowship from the Plastics Institute of America. Various polymers used in this work were kindly supplied by Bayer Corporation and Mitsubishi Engineering Plastics Corporation.

References

[1] Grabowski TS. US Patent, 3,130,177, 1964 (to Borg-Warner Corp.).
[2] Greco R, Sorrentino A. Adv Polym Tech 1994;13:249.
[3] Lombardo BS, Keskkula H, Paul DR. J Appl Polym Sci 1994;54:1697.
[4] Ishikawa M, Chiba I. Polymer 1990;31:1232.
[5] Greco R. In: Martuscelli E, Musto P, Ragosta G, editors. Advanced routes for polymer toughening, ch. 9. Amsterdam: Elsevier, 1996.
[6] Callaghan TA, Takakuwa K, Paul DR, Padwa AR. Polymer 1993;34:3796.
[7] Kim CK, Paul DR. Polymer 1992;33:4941.
[8] Mendelson RA. J Polym Sci, Polym Phys Ed 1985;23:1975.
[9] Guest MJ, Daly JH. Eur Polym J 1989;25:985.
[10] Guest MJ, Daly JH. Eur Polym J 1990;26:603.
[11] Keitz JD, Barlow JW, Paul DR. J Appl Polym Sci 1984;29:3131.
[12] Quintens D, Groeninckx G, Guest M, Aerts L. Polym Eng Sci 1990;30:1474.
[13] Kim WN, Burns CM. Polym Eng Sci 1988;28:1115.
[14] Janarthanan V, Stein RS, Garrett PD. J Polym Sci: Part B: Polym Phys 1993;31:1995.
[15] Skochdopole RE, Finch CR, Marshall J. Polym Eng Sci 1987;27:627.
[16] Wu J, Shen S, Chang F. J Appl Polym Sci 1993;50:1379.
[17] Cheng TW, Keskkula H, Paul DR. J Appl Polym Sci 1992;45:1245.
[18] Quintens D, Groeninckx G, Guest M, Aerts L. Polym Eng Sci 1990;30:1484.
[19] Kelnar I, Fortelny I. J Polym Eng 1995;14:269.
[20] Macosko CW, Guegan P, Khandpur AK, Nakayama A, Marechal P, Inoue T. Macromolecules 1996;29:5590.
[21] Majumdar B, Paul DR, Oshinski AJ. Polymer 1997;38:1787.
[22] Sundararaj U, Macosko CW. Macromolecules 1995;28:2647.
[23] Fortelny I, Zivny A. Polymer 1995;36:4113.
[24] Elmendorp JJ, van der Vegt AK. In: Utracki LA, editors. Two-phase polymer systems, ch. 6. Munich: Carl Hanser, 1991.
[25] Chen CC, White JL. SPE ANTEC '91, 1991:969.
[26] Utracki, LA. Polymer alloys and blends. Munich: Carl Hanser/ Dusseldorf: VDI Verlag, 1989.
[27] Sondergaard K, Lyngaae-Jorgensen J. In: Nakatani AI, Dadmun MD, editors. Flow-induced structure in polymers. Washington, DC: American Chemical Society, ch. 12:1995.
[28] Willis JM, Caldas V, Favis BD. J Mater Sci 1991;26:4742.
[29] Wildes GS, Harada T, Keskkula H, Janarthanan V, Padwa AR, Paul DR. Submitted to Polymer.
[30] Favis BD, Willis JM. J Polym Sci: Part B: Polym Phys 1990;28:2259.
[31] White JL, Min K. Adv Polym Tech 1985;5:225.
[32] Tokita N. Rubber Chem Technol 1977;50:292.
[33] Favis BD, Chalifoux JP. Polymer 1988;29:1761.
[34] Min K, White JL, Fellers JF. Polym Eng Sci 1984;24:1327.
[35] Min K, White JL, Fellers JF. J Appl Polym Sci 1984;29:2117.
[36] Utracki LA, Dumooulin MM, Toma P. Polym Eng Sci 1986;26:34.
[37] Willis JM, Favis BD. Polym Eng Sci 1988;28:1416.
[38] Wu S. Polym Eng Sci 1987;27:335.
[39] Cimmino C, D'Orazio L, Greco R, Maglio G, Malinconico M, Mancarella C, Martuscelli E, Palumbo R, Ragosta C. Polym Eng Sci 1984;24:48.
[40] Majumdar B, Keskkula H, Paul DR, Harvey NG. Polymer 1994;35:4263.
[41] Wildes GS, Keskkula H, Paul DR. Submitted to Polymer.
[42] Dharmarajan NR, Yu TC. Plast Eng 1996;LII:33.
[43] Fortelny I, Kovar J, Stephan MJ. Elast Plast 1996;28:106.
[44] Janssen JMH, Meijer HEH. Polym Eng and Sci 1987;35:1766.
[45] Chen CC, Fontan E, Min K, White J. Polym Eng Sci 1988;28:69.
[46] Taylor GI. Proc R Soc 1932;A 138:41.
[47] Taylor GI. Proc R Soc 1934;A 146:501.
[48] Grace HP. Chem Eng Commun 1982;14:225.
[49] Karam HJ, Bellinger JC. Ind Eng Chem Fundam 1986;167:241.
[50] Tavgac T. PhD Dissertation, University of Houston, 1972.
[51] Bartok W, Mason SG. J Colloid Sci 1959;14:13.
[52] van Oene HJ. J Colloid Sci 1972;40:448.
[53] van Oene HJ. In: Paul DR, Newman S, editors. Polymer blends, vol. 1, New York: Academic Press, 1978.
[54] Mirabella FM, Barley JS. J Polym Sci Polym Phys Ed 1995;33:2281.
[55] von Smoluchowski MZ. Physik Z 1916;17:557.
[56] von Smoluchowski MZ. Z Physik Chem 1917;92:129.
[57] Jang BZ, Uhlmann DR, van den Sande JV. Rubber Chem Technol 1984;57:291.
[58] Meier DJ. Submitted to Polymer.
[59] Utracki LA, Shi ZH. Polym Eng Sci 1992;32:1824.
[60] Mirabella FM. J Polym Sci, Polym Phys Ed 1994;32:1205.
[61] Chesters AK. Trans I Chem Eng, Part A 1991;69:259.
[62] Crist B, Nesarikar AR. Macromolecules 1995;28:890.
[63] Beysens DA. Physica A 1997;239:329.
[64] Elmendorp JJ, Van der Vegt AK. Polym Eng Sci 1986;26:418.
[65] Elmendorp JJ, Van der Vegt AK. Polym Eng Sci 1986;26:1332.
[66] Fortelny I, Zivny A. Polym Eng Sci 1995;35:1872.
[67] Chen CC, White JL. Polym Eng Sci 1993;33:923.
[68] Ito Y, Hiromi O, Yasuyuki I, Ohtani H, Shin T. Polym J 1996;28:1090.
[69] Hale W, Keskkula H, Paul DR. Submitted to Polymer.
[70] Chamot EM, Mason CW. Handbook of chemical microscopy. London: Wiley, 1983.
[71] Irani RR, Callis CF. Particle size: measurement, interpretation and application. New York: Wiley, 1963.
[72] Roland CM, Bohm GGA. J Polym Sci, Polym Phys Ed 1984;22:79.
[73] Kresler J, Higashida N, Inoue T, Heckmann W, Seitz F. Macromolecules 1993;26:2090.
[74] Burton RH, Folkes MJ, Narth KA, Keller AJ. J Mater Sci 1983;18:315.
[75] de Gennes PG. Rev Mod Phys 1985;57:827.
[76] Oshinski AJ, Keskkula H, Paul DR. Polymer 1992;33:268.
[77] Triacca VJ, Ziaee S, Barlow JW, Keskkula H, Paul DR. Polymer 1991;32:1401.
[78] Merfeld GD, Karim A, Majumdar B, Paul DR. Submitted to Polymer.